Molecular Magnets Based on Nickel(II) Complexes with 3-Imidazoline Nitroxides and Alcohols

Vladimir N. Ikorskii, Victor I. Ovcharenko,* Yurii G. Shvedenkov, Galina V. Romanenko, Sergei V. Fokin, and Renad Z. Sagdeev

International Tomography Center, Siberian Branch of Russian Academy of Sciences, Institutskaya 3a, Novosibirsk, 630090, Russia

Received February 19, 1998

Crystallization of heterospin bischelate NiL_2, where L is deprotonated nitroxide 4-(3′,3′,3′-trifluoromethyl-2′-oxopropylidene)-2,2,5,5-tetramethyl-3-imidazoline-1-oxyl, with alcohols allows a logical assembly of layered $[NiL_2(CH_3OH)_2$ (**1**) and $NiL_2(C_2H_5OH)_2$ (**2**)] or frame compounds $[NiL_2(HO(CH_2)_4OH)$ (**3**) and $NiL_2(HO(CH_2)_5OH)$ (**4**)]. The structures of complexes **1**, **2**, and **4** have been determined. Crystal data: **1**, monoclinic, space group $P2_1/c$, $a = 8.929(2)$ Å, $b = 15.773(3)$, $c = 11.518(2)$, $\beta = 118.84(1)°$, $Z = 2$; **2**, monoclinic, space group $P2_1/c$, $a = 9.923(5)$ Å, $b = 15.992(5)$ Å, $c = 11.486(2)$ Å, $\beta = 120.63(3)°$, $Z = 2$; **4**, monoclinic, space group $C2/c$, $a = 21.028(4)$ Å, $b = 10.943(2)$, $c = 14.405(3)$, $\beta = 110.61(3)°$, $Z = 4$. The structure of **3** is very close to the structure of **4** and has been reported earlier. Robust H-bonding between the OH groups of the coordinated alcohols and the >N−•O groups of the neighboring fragments NiL_2 leads to the formation of polymeric layers in the solid. At the same time, hydrogen bonds form effective channels for magnetic interactions >N−•O···H−O^R−Ni^{2+}−^{R}O−H···O•−N<. The magnetic phase transition to the weak ferromagnetic state below 7 K is inherent in **1**−**4**. For **2** and **4**, this transition is induced by the external magnetic field that correlates with the elongation of Ni−^{R}O and ^{R}O···O•− distances in the exchange channels >N−•O···H−O^R−Ni^{2+}−^{R}O−H···O•−N< in solids **2** and **4** compared to **1** and **3**. It has been found that magnetic ordering occurs only within the polymeric layers formed due to multiple hydrogen bonds. Investigation of the anisotropy of magnetic susceptibility performed on large single crystals of **1**−**4** revealed an essentially different ordering of the magnetic moments of magnetic sublattices in **1**, **2** and in **3**, **4**.

Introduction

In the past decade, a large group of molecular ferromagnets based on metal-containing heterospin compounds of different classes have been created. Among them are radical ion salts,[1,2] metal cyanides,[3−7] heterometallic compounds with polydentate organic ligands,[8,9] and compounds of paramagnetic metal ions with stable nitroxides.[10−12] Effective techniques for designing *n*-dimensional heterospin systems capable of cooperative magnetic ordering have been developed,[10−14] and promising applications of molecular ferromagnets as technical magnets are envisaged.[2,13] Recent progress in the field of molecular ferromagnets permits not only selective design of individual polymeric heterospin molecules, but also control of the packing of these molecules in the crystal.[14] 1-, 2-, and 3-dimensional heterospin structures are valuable models for theoretical and experimental investigations of magneto-structural correlations. To continue our studies on molecular ferromagnets based on metal complexes with stable nitroxides, we would like to draw attention to using hydrogen bonding in the design of 2-D and 3-D heterospin molecular magnets based on Ni(II) complexes with 3-imidazoline nitroxides and alcohols. The group of compounds under discussion includes layered polymer and frame complexes $NiL_2(CH_3OH)_2$ (**1**), $NiL_2(C_2H_5OH)_2$ (**2**), $NiL_2(HO(CH_2)_4OH)$ (**3**) and $NiL_2(HO(CH_2)_5OH)$ (**4**), where L is a deprotonated nitroxide 4-(3′,3′,3′-trifluoromethyl-2′-oxopropylidene)-2,2,5,5-tetramethyl-3-imidazoline-1-oxyl and $HO(CH_2)_4OH$ and $HO(CH_2)_5OH$ are 1,4-butanediol and 1,5-pentanediol, respectively. Compounds **1**−**4** are actually the first heterospin molecular magnets in which formation of a 2-D or 3-D structure is promoted by hydrogen bonding between the coordinated alcohol molecules. Simultaneously, the intermolecular hydrogen bonds of the coordinated alcohol molecules form effective exchange channels >N−•O···H−O^R−Ni^{2+}−^{R}O−H···O•−N< in the solids, which leads to cooperative ordering of spins below the critical temperature. It is noteworthy that the ever growing number of heterospin molecular ferromagnets

* To whom correspondence should be addressed.

(1) Miller, J. S.; Epsttein, A. J.; Reiff, W. M. *Science* **1988**, *240*, 40.
(2) Miller, J. S. *Adv. Mater.* **1994**, *6* (4), 322.
(3) Manriquez, J. M.; Yee, G. T.; McLean, R. S.; Epstein, A. J.; Miller, J. S. *Science* **1991**, *252*, 1415.
(4) Ferlay, S.; Mallah, T.; Ouahés, R.; Veillet, P.; Verdaguer, M. *Nature* **1995**, *378*, 701.
(5) Entley, W. R.; Girolami, G. S. *Science* **1995**, *268*, 397.
(6) Kahn, O. *Nature* **1995**, *378*, 667.
(7) Mallah, T.; Thirébaut, S.; Verdaguer, M.; Veillet, P. *Science* **1993**, *262*, 1554.
(8) Nakatani, K.; Carriat, J. Y.; Journaux, Y.; Kahn, O.; Lloret, F.; Renard, J. P.; Pei, Yu; Sletten, J.; Verdaguer, M. *J. Am. Chem. Soc.* **1989**, *111*, 5739.
(9) Stumpf, H. O.; Ouahab, L.; Pei, Yu; Grandjean, D.; Kahn, O. *Science* **1993**, *261*, 447.
(10) Caneschi, A.; Gatteschi D.; Rey, P. *Progr. Inorg. Chem.* **1991**, *39*, 331.
(11) Inoue, K.; Hayamizu, T.; Iwamura, H.; Hashizume, D.; Ohashi, Y. *J. Am. Chem. Soc.* **1996**, *118*, 1803.
(12) Volodarsky, L. B.; Reznikov, V. A.; Ovcharenko, V. I. *Synthetic Chemistry of Stable Nitroxides*; CRC Press: Boca Raton, FL, 1994.
(13) Miller, J. S.; Epstein, A. J. Angew. *Chem., Int. Ed. Engl.* **1994**, *33*, 385.
(14) Kahn, O. *Molecular Magnetism*; VCH: New York, 1993.

S0020-1669(98)00184-0 CCC: $15.00
Published on Web 08/07/1998

Table 1. Crystallographic Data for **1**, **2**, and **4**

	$NiL_2(CH_3OH)_2$ **1**	$NiL_2(C_2H_5OH)_2$ **2**	$NiL_2(HO(CH_2)_5OH)$ **4**
chemical formula	$C_{22}H_{34}F_6N_4NiO_6$	$C_{24}H_{38}F_6N_4NiO_6$	$C_{25}H_{38}F_6N_4NiO_6$
fw	623.24	651.29	663.30
space group	$P2_1/c$	$P2_1/c$	$C2/c$
V (Å^3)	1421.0(5)	1568.4(12)	3102.6(10)
Z, d_{calc}, g/cm^3	2, 1.457	2, 1.379	4, 1.420
a, Å	8.929(2)	9.923(5)	21.028(4)
b, Å	15.773(3)	15.992(5)	10.943(2)
c, Å	11.518(2)	11.486(5)	14.405(3)
β, deg	118.84(1)	120.63(3)	110.61(3)
μ(Mo K$_\alpha$), mm^{-1}	0.764	0.695	0.704
R1[a] ($I > 2\sigma_I$)	0.0496	0.0663	0.0381
wR2[a] ($I > 2\sigma_I$)	0.1312	0.1606	0.0810

[a] $R1 = \sum||F_o| - |F_c||/\sum|F_o|$, $wR2 = [\sum[w(F_o^2 - F_c^2)^2]/\sum(w(F_o^2)^2)]^{1/2}$.

poses an important question about the character of ordering of magnetic moments below the critical temperature. This problem may not be solved by investigating polycrystalline samples and demands detailed studies of the anisotropy of magnetic susceptibility of single crystals of the compounds. This study was performed by us, because we were able to grow single crystals of **1**−**4** to sufficient size. A complex pattern of magnetic ordering, not observed previously for molecular magnets, was found.

Experimental Section

Syntheses of the Complexes and Growing Single Crystals. Single crystals **4** were grown from an acetone solution of NiL_2, previously obtained by the procedure published elsewhere,[15] with an addition of a 1,5-pentanediol excess. The initial concentration of NiL_2 in the solution was up to 20 mmol/L, and the ratio of $NiL_2/HO(CH_2)_5OH$ was 1:10. At higher concentrations of NiL_2 in the solution or with a larger excess of 1,5-pentanediol, or when the solution was jerked during the growth of single crystals, finely dispersed $NiL_2(HO(CH_2)_5OH)$ separated out as a solid. Below we give a typical procedure for growing single crystals of $NiL_2(HO(CH_2)_5OH)$ suitable for an X-ray diffraction analysis. NiL_2 (3 g) was dissolved with heating in 300 mL of acetone. The resulting solution was filtered, and 1,5-pentanediol (5 g) was added to the filtrate. The flask with the solution was kept loosely stoppered at room temperature. After 1 or 2 weeks, acetone gradually evaporated, and perfectly shaped bright green single crystals of $NiL_2(HO(CH_2)_5OH)$ suitable for an X-ray diffraction analysis separated out as solids. The crystals were filtered off, washed with water, and dried with an air current. Anal. Calcd for $C_{25}H_{38}F_6N_4O_6Ni$: C, 45.26; H, 5.77; N, 8.44; Ni, 8.85. Found: C, 45.12; H, 5.98; N, 8.47; Ni, 8.88. When left in solution for several weeks, the crystals grow to a significantly larger size (from several millimeters to 1 or 2 cm along the longest edge). A few single crystals were taken for a magnetochemical experiment; for these crystals, indices of faces were previously determined on an Enraf Nonius CAD4 automatic single-crystal diffractometer.

Complexes 1, **2**, and **3** were synthesized as in refs 16 and 17. Single crystals of $NiL_2(HO(CH_2)_4OH)$ (**3**) suitable for a magnetochemical experiment were grown by the same procedure as for single crystals of **4**, and single crystals of $NiL_2(CH_3OH)_2$ (**1**) and $NiL_2(C_2H_5OH)_2$ (**2**) were grown by keeping methanol and ethanol solutions of NiL_2, respectively, for many months at room temperature. Large single crystals **1**−**4** are sufficiently stable both under the layer of the mother solution and when stored in normal conditions. When stored in alcohol solutions for several years, NiL_2 molecules remain unchanged. Due to this, large (>1 cm) single crystals may be grown by slow crystallization of compounds during prolonged storage of the corresponding oversaturated mother solutions of NiL_2.

Magnetic measurements for single crystals were carried out on an MPMS-5S SQUID magnetometer (Quantum Design) in the temperature range of 2−300 K and with a magnetic field strength of up to 10 kG. The crystal holder was a Teflon glass (diameter 5.4 mm, height 2.5 mm, mass 62 mg), which fitted tightly in a standard plastic tube. For single crystals 1−5 mg in mass, a relationship between the crystallographic axes and the external habit was preliminarily determined, whereupon the samples were fixed at the bottom of the glass with the aid of a thin layer of vacuum lubricant. The crystal was orientated relative to the direction of the magnetic field in three mutually perpendicular directions by varying the position of the crystal in the tube. The oriented crystal was cooled to 2 K. The magnetic measurements were performed by gradually heating the sample to 300 K. The crystal was then taken out, turned, and cooled again. This procedure was repeated several times. For each direction, magnetic susceptibility measurements were preliminarily carried out for an empty sample holder. The values found in these measurements were then taken into account to establish the true magnetic susceptibility of the sample.

The molar magnetic susceptibility was calculated using corrections for the diamagnetism of the complex and for the temperature-independent paramagnetism of the Ni(II) ion, which is 190 emu/mol.

Crystal Data Collection and Refinement of the Structures. Crystal data and details of data collection are given in Table 1. All crystals (green prisms) were mounted on glass fibers with a glue at room temperature. Data collection was performed on a SYNTEX $P2_1$ X-ray diffractometer (**1** and **2**) and Enraf Nonius CAD-4 X-ray diffractometer (**4**) (Mo Kα radiation, $\lambda = 0.710\,69$ Å). Data were collected in the θ range 2.40−25.32° (**1**), 2.39−27.47° (**2**), and 2.13−26.96° (**4**) with three control reflections collected for every 100 reflections. Lorentz and polarization corrections were applied to 5082 ($R_{int} = 0.0473$) reflections for **1**, 2770 ($R_{int} = 0.0898$) for **2**, and 3148 ($R_{int} = 0.0221$) for **4**. Corrections for absorption were made experimentally using transmission curves for **1**, **2**, and **4**. All structures were solved by direct methods (SHELXS program package, SHELXS86). Further least-squares full-matrix anisotropic refinement (SHELXL97) for all nonhydrogen atoms and isotropic for hydrogen atoms yielded final R and R_w indices and GOOF of 4.96%, 13.12%, 1.069; 6.63%, 16.06%, 1.143; and 3.11%, 7.94%, 0.964 for **1**, **2**, and **4**, respectively. Tables containing full listings of atomic positions, anisotropic displacement parameters, and hydrogen atom positions are available as Supporting Information. Full structural data of **3** were given elsewhere,[16] and the results of the preliminary structure investigation of **1** and **2** were presented elsewhere.[17]

Results and Discussion

Description of the Structures of 1−4. The similarity between the structures of **1**−**4** is an important point of this investigation. In all complexes, the centrosymmetric square

(15) Ovcharenko, V. I.; Vostrikova, K. E.; Podoplelov, A. V.; Sagdeev, R. Z.; Romanenko, G. V.; Ikorskii, V. N. *Polyhedron* **1994**, *13*, 2781.
(16) Romanenko, G. V.; Ikorskii, V. N.; Fokin, S. V.; Ovcharenko, V. I. *Zh. Strukt. Khim.* **1997**, *38*, 930.
(17) Ovcharenko, V. I.; Vostrikova, K. E.; Romanenko, G. V.; Ikorskii, V. N.; Podberezskaya, N. V.; Larionov, S. V. *Dokl. Akad. Nauk SSSR* **1989**, *306*, 115.

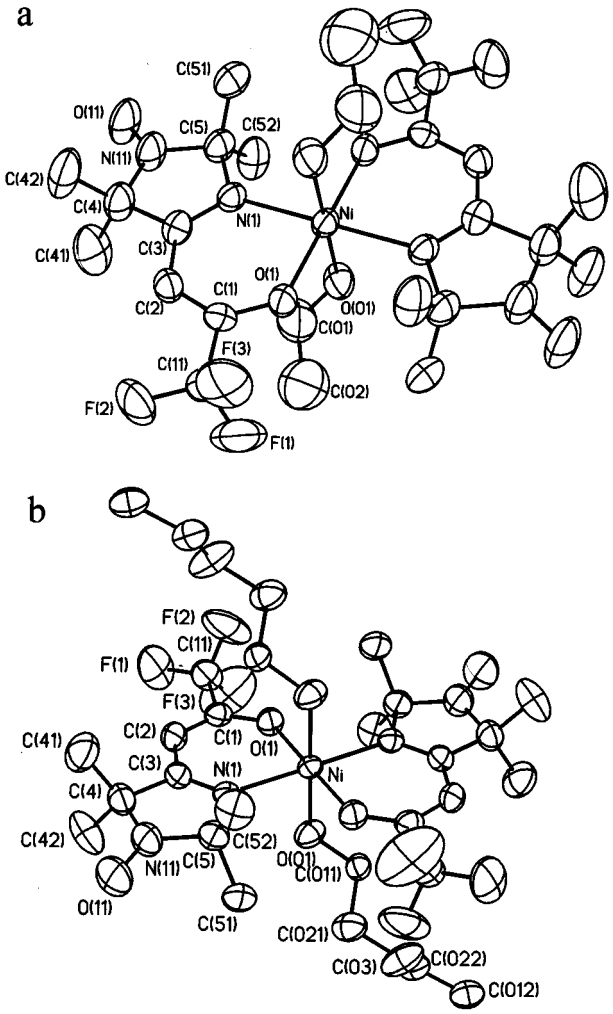

Figure 1. ORTEP drawing of the $NiL_2(C_2H_5OH)_2$ molecule (a) and the fragment of $NiL_2(HO(CH_2)_5OH)$ structure (b) with the atomic numbering scheme. The atom numbers in $NiL_2(CH_3OH)_2$ and $NiL_2(HO(CH_2)_4OH)$ are the same. The ellipsoids are drawn at the 50% probability level, and hydrogen atoms are removed for clarity.

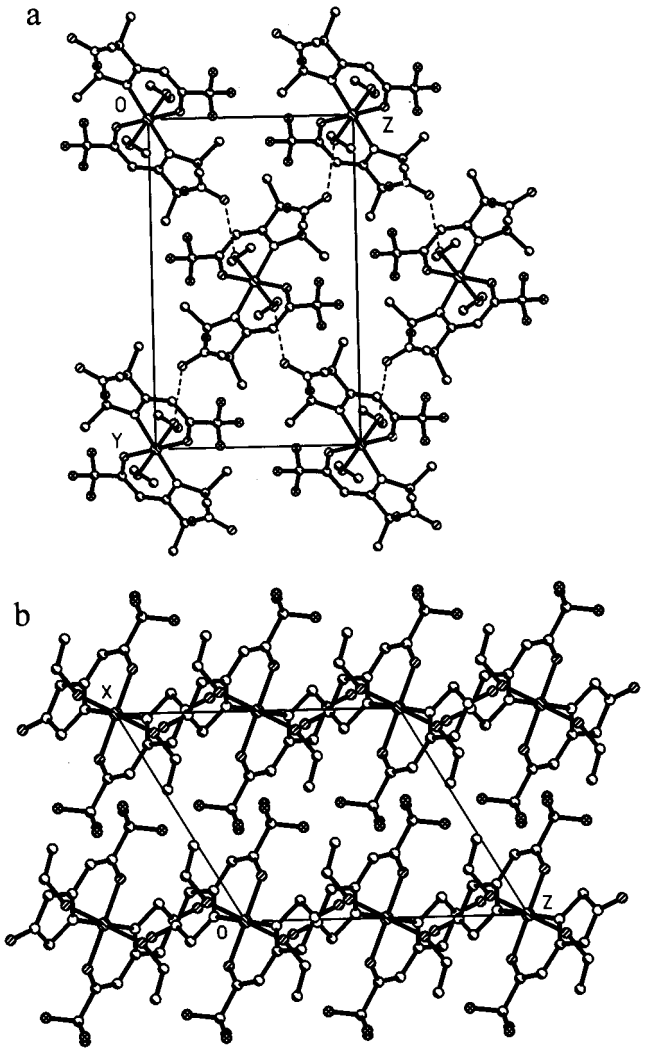

Figure 2. Crystal structure projection of $NiL_2(C_2H_5OH)_2$ onto (100) (a) and (010) (b) planes. Methyl groups are omitted on (b) for clarity.

environment of the nickel atom formed by the N and O donor atoms of the two bidentate-coordinated ligands L is made octahedral by the oxygen atoms of the OH groups of alcohol molecules. Figure 1 gives the structure and the numbering scheme of a molecular fragment for **2** and **4**, which are analogous to those for **1** and **3**. The average Ni−O, Ni−N, and Ni−OH bond lengths for **1**−**4** are 1.999(6), 2.131(11), and 2.115(16) Å, respectively; the NNiO angles in the chelate rings are, on the average, 88.3(3)°. The N−O bond lengths in the nitroxyl group are typical for nitroxides and are 1.275(2) Å (average). Selected bond lengths and bond angles and parameters of hydrogen bonds and shortest F···F interlayer contacts in **1**−**4** are given in Table 2.

The $NiL_2(CH_3OH)_2$ and $NiL_2(C_2H_5OH)_2$ molecular fragments in the structure of **1** and **2** are linked with each other by tight hydrogen bonds, O···HO between the coordinated OH groups of alcohols and the N−•O groups of L. This leads to formation of layers (Figure 2a) parallel to the (100) plane. In complexes **3** and **4,** the coordinated 1,4-butanediol and 1,5-pentanediol molecules also link the NiL_2 fragments into polymeric layers via the hydrogen bonds of OH groups, which are analogous to the hydrogen bonds in the polymer layers of **1** and **2**. The hydrocarbon chains -$(CH_2)_4$- and -$(CH_2)_5$-, in turn, connect the polymer layers into a framework (Figure 3).

The coordinated alcohol molecules involved in hydrogen bonds are tightly held in solids **1**−**4**. Complexes with glycols **3** and **4**, possessing a frame structure, do not show pronounced decomposition even when heated in a vacuum to 100 °C. When stored in normal conditions, their composition and properties do not change for several years. Complexes with methanol and ethanol **1** and **2** are also stable in normal conditions for long time (1 or 2 years) provided that they are perfect large crystals and are stored in a closed vessel. Finely crystalline powders **1** and **2** are less stable in normal conditions. When stored in open flasks, they gradually lose alcohol and are transformed into NiL_2. (Solid NiL_2 exists as two polymorphs. Their crystal structures and magnetic properties were described elsewhere.[18]) This process may be promoted by heating the $NiL_2(CH_3OH)_2$ and $NiL_2(C_2H_5OH)_2$ powders in a vacuum at 60−70 °C. The smaller and less perfect are the crystals of the complexes, the faster is the loss of alcohol. The TG curves in the temperature range 70−115 °C for $NiL_2(CH_3OH)_2$ and 55−95 for $NiL_2(C_2H_5OH)_2$ show marked steps of removal of alcohol molecules, corresponding to the endo effect on the DTA curves. Complete elimination of alcohol molecules during the heating of the complexes is confirmed by a comparison of the IR spectra of specially synthesized $NiL_2(CD_3OD)_2$ and $NiL_2(C_2H_5OD)_2$ with

(18) Ovcharenko, V. I.; Romanenko, G. V.; Ikorskii, V. N.; Musin, R. N.; Sagdeev, R. Z. *Inorg. Chem.* **1994**, *33*, 3, 3370.

Table 2. Selected Bond Lengths (Å) and Angles (deg) for **1**−**4**

	$NiL_2(CH_3OH)_2$ **1**	$NiL_2(C_2H_5OH)_2$ **2**	$NiL_2(HO(CH_2)_4OH)$ **3**	$NiL_2(HO(CH_2)_5OH)$ **4**
Ni−O(1)	1.996(3)	2.000(4)	2.006(1)	1.992(1)
Ni−O(01)	2.094(4)	2.124(4)	2.112(1)	2.131(2)
Ni−N(1)	2.127(3)	2.129(4)	2.121(2)	2.147(1)
N(11)−O(11)	1.278(5)	1.274(6)	1.273(2)	1.275(2)
O(1)−Ni−O(01)	91.1(1)	90.6(2)	89.43(6)	88.66(6)
O(1)−Ni−N(1)	88.1(1)	88.7(2)	88.04(5)	88.42(5)
O(01)−Ni−N(1)	90.1(1)	90.3(2)	90.01(6)	90.15(6)
O(11)−N(11)−C(4)	124.3(3)	123.9(5)	123.2(2)	123.3(2)
O(11)−N(11)−C(5)	122.1(3)	122.4(5)	122.8(2)	122.8(2)
C(4)−N(11)−C(5)	113.5(3)	113.3(4)	113.9(2)	113.9(2)
C(01)−O(01)−Ni	125.8(5)	129.4(5)	127.8(1)	124.9(2) 126.4(2)
C(01)−O(01)−H(01)	108(4)	110(4)	110(2)	103(2) 109(2)
Ni−O(01)−H(01)	120(4)	118(4)	122(2)	123(2)
		H−bond Parameters		
O(01)···O(11′)	2.730(4)	2.785(6)	2.736(2)	2.872(2)
O(01)−H(01)	0.73(4)	0.86(7)	0.77(2)	0.69(3)
H(01)···O(11′)	2.02(3)	1.95(7)	2.03(2)	2.26(3)
O(01)H(01)O(11′)	166(4)	162(6)	153(2)	149(3)
		Interlayer Contacts		
F···F	2.875(6)	3.028(9)	3.185(2)	4.176(3)

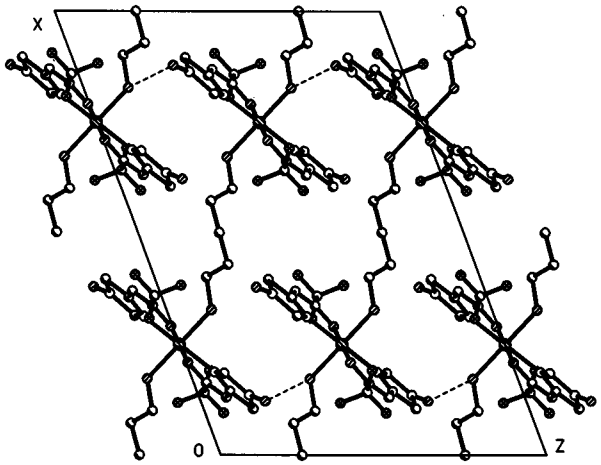

Figure 3. Projection of the crystal structure of $NiL_2(HO(CH_2)_5OH)$ onto (010) plane. $HO(CH_2)_5OH$ molecules connect layers with one another. Only one configuration of the $HO(CH_2)_5OH$ molecule is shown, and methyl groups are omitted for clarity.

the spectrum of the product of their prolonged storage in a vacuum at 60−70 °C, which is identical to the IR spectrum of NiL_2. In the IR spectra of the product of thermal storage, the absorption bands of the alcohol molecules ν(O−D) at 2487 and 2500 cm^{-1}, typical for $NiL_2(CD_3OD)_2$ and $NiL_2(C_2H_5OD)_2$, respectively, are lacking. Using deuterated alcohols makes it convenient to monitor the presence of alcohol molecules in the solid in the range 2450−2550 cm^{-1}, in which $NiL_2(ROD)_2$ have no other absorption bands. If NiL_2 powder is kept in methanol or ethanol vapor in an desiccator for a day, it is quantitatively transformed into $NiL_2(CH_3OH)_2$ or $NiL_2(C_2H_5OH)_2$, respectively. Thus alcohol molecules are tightly held in solids **1**−**4**. For this reason, preparation of single crystals **1**−**4** for magnetochemical measurements did not require any special precautions, and single crystals **1**−**4** did not change their mass or other physical characteristics during magnetochemical measurements.

It is noteworthy that the alcohols 1,4-butanediol and 1,5-pentanediol were chosen on purpose for a transition from layered to frame structures. Figure 2a shows the structure of a polymer layer in $NiL_2(C_2H_5OH)_2$, whose motif is typical for all compounds under discussion, and Figure 2b gives a schematic view of the layers along the (010) direction. Figure 2b clearly shows that the hydrocarbon "tails" of alcohol molecules, along with CF_3 groups, are directed toward the interlayer space. Thus, a frame structure may be realized by "sewing" together the hydrocarbon tails of alcohol molecules, which was actually done using 1,4-butanediol and 1,5-pentanediol (Figure 3). As would be expected, a transition from 1,4-butanediol to 1,5-pentanediol increases the interlayer distances; this is evident from an increase in F···F interlayer contacts (Table 2). Further expansion of the methylene chain $-(CH_2)_n-$, increasing the interlayer distances, seemed undesirable, and glycols with a shorter hydrocarbon chain, 1,2-ethanediol and 1,3-propanediol, may not be used for building frame structures, as they may be coordinated by the metal atom in a bidentate way to form 5- and 6-membered chelate rings, respectively.[19]

An analysis of bond lengths and angles in the polymer layers of **1**−**4** revealed two parameters in which structures **1** and **3** show statistically significant difference from structures **2** and **4** and which deserve special attention. These are Ni−O(01) and O(01)···O(011′) distances, which are shorter by 0.01−0.02 and 0.05−0.13 Å, respectively, in **1** and **3** relative to **2** and **4** (Table 2). The Ni−O(01) and O(01)···O(011′) bonds are involved in the $>N-^{\bullet}O\cdots H-O^{R}-Ni^{2+}$ exchange channel and their change may considerably affect the magnetic properties of the com-

(19) Complexes with 1,2-ethanediol and 1,3-propanediol $NiL_2(HO(CH_2)_2OH)$ and $NiL_2(HO(CH_2)_3OH)$ were isolated using a synthetic procedure analogous to that applied for the preparation of **3**, **4**. The complexes had satisfactory analysis data. When heated in air, they are transformed into NiL_2 as $NiL_2(CH_3OH)_2$ and $NiL_2(C_2H_5OH)_2$, but the temperature range of removal of 1,2-ethanediol and 1,3-propanediol (120−170 °C) is considerably higher than that of methanol and ethanol. The diffractograms of $NiL_2(HO(CH_2)_2OH)$ and $NiL_2(HO(CH_2)_3OH)$ differ greatly and have no lines in common with the diffractograms of **1**−**4**, which indicates that the structures of these compounds differ considerably from those of **1**−**4**. Contrary to **1**−**4**, for $NiL_2(HO(CH_2)_2OH)$ and $NiL_2(HO(CH_2)_3OH)$, magnetic susceptibility is independent of the value of magnetic field over the whole temperature range of measurements. The magnetic properties of these compounds are trivial and well fitted by the model of quasiisolated exchange clusters[25] with $g = 2.20$, $J = 7.2$ cm^{-1}, $J'z = -0.1$ cm^{-1} for $NiL_2(HO(CH_2)_2OH)$ and $g = 2.25$, $J = 8.4$ cm^{-1}, $J'z = -0.5$ cm^{-1} for $NiL_2(HO(CH_2)_3OH)$.

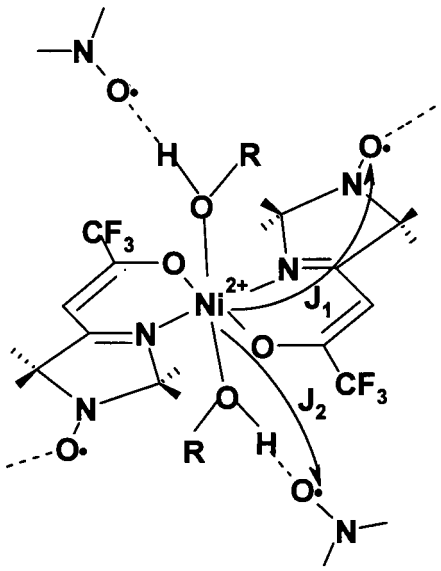

Figure 4. Exchange channels J_1 and J_2.

pounds, as, indeed, was found and is discussed below. Also, we note that the shortest F···F interlayer contacts in **1** and **2** are 2.875(6) and 3.030(6) Å, respectively. These contacts are almost equal or slightly exceed the sum of van der Waals radii of the two fluorine atoms (1.40 Å). For **3** and **4,** these distances are considerably longer (Table 2), which is also important to note before discussing the magnetic properties of the complexes. In conclusion we also note that the bond lengths and angles in the bischelate fragment NiL_2 in **1**-**4** are close to those in the previously investigated polymorphs of NiL_2 and $NiL^{(Cl)}{}_2(CH_3OH)_2$, where $L^{(Cl)}$ is an analogue of L containing a chlorine atom in the γ-position of the enaminoketone group.[18,20]

Magnetic Properties. For polycrystalline complexes **1**−**3**, the magnetic transition was found at 4−6 K.[16,17,21] Figure 4 shows a scheme of exchange channels forming exchange interactions between unpaired electrons in a layer. The indirect intramolecular exchange interactions J_1 are ferromagnetic and are of the order of 10 cm^{-1}.[15,21,22] The exchange interactions of the J_2 channel are antiferromagnetic; their magnitude exceeds the interaction energies of the J_1 channel, as indicated by an increase in the effective magnetic moment when the temperature increases above the magnetic transition temperature. Below 6 K, specific magnetic ordering is observed for **1**−**4.** The character of the ordering allows one to attribute the compounds to antiferromagnets with weak ferromagnetism. We observed two types of magnetic transition to the weakly ferromagnetic state depending on the alcohol molecule entering into the compound. One of these transitions (for **2** and **4**) is induced by the external magnetic field. Magnetic ordering in **1**−**4**, unlike weakly ferromagnetic compounds, is determined by two essentially different magnetic subsystems related by exchange interaction. The first subsystem is the magnetic subsystem of nickel ions, possessing pronounced anisotropic properties and subject to the crystalline anisotropy effect. Under certain conditions, this subsystem can independently go over to the weakly ferromagnetic state. The second subsystem is the subsystem of unpaired electrons of >N−•O groups, which has much less significant anisotropy. For this subsystem, this type of ordering is not inherent and was not observed experimentally until recently. Therefore, for the heterospin complexes discussed here, below the magnetic transition temperature one can expect a significant difference in the magnetic ordering of the magnetic subsystem of radicals and the magnetic subsystem of Ni(II) ions relative to known compounds with weak ferromagnetism containing identical paramagnetic centers.[23] For complexes of paramagnetic ions of transition metals with stable organic radicals, this situation must be regarded as the general case. Due to this, studies on the anisotropy of the magnetic properties of single crystals **1**−**4** above and below the magnetic transition temperature to establish the structure of their magnetic ordering are of special interest.

Magnetic Properties below T_N. The field dependences of magnetization of single crystals **1** and **3** at 2 K for different directions are presented in Figure 5. Designations of the *y* and *z* axes used in the discussion of the magnetic properties of the single crystals coincide with the crystallographic directions *y* and *z* given in Figure 2a; the *x* axis is perpendicular to the *yz* plane and differs from the crystallographic direction *x* by an angle [β(Table 1) − 90]°. As one can see in Figure 5, along the *y* direction in crystals **1** and **3** (Figure 2a) magnetization depends on the magnetic field **H**[24] as

$$M = M_S + \chi_\perp \mathbf{H} \qquad (1)$$

where M_S is spontaneous ferromagnetic moment, and $\chi_\perp$ is paramagnetic susceptibility; this dependence is typical for weakly ferromagnetic compounds. Along the *x* and *z* directions, magnetization $M \rightarrow 0$ when $\mathbf{H} \rightarrow 0$.

For crystals **2** and **4**, dependence (1) for the *y* direction appears only in the critical magnetic field $\mathbf{H}_C$ (Figure 6). When the temperature increases, $\mathbf{H}_C$ decreases to zero at the magnetic transition temperature T_N. The value of the critical field $\mathbf{H}_C$ at a definite temperature was determined from the maximum of the derivative $dM(\mathbf{H})/d\mathbf{H}$. Figures 7 and 8 present the temperature dependencies of the weakly ferromagnetic spontaneous moment M_S and the critical field $\mathbf{H}_C$ for single crystals **1**−**4**.

Magnetic Susceptibility at T_N. Figures 9 and 10 show the experimental dependencies of magnetic susceptibility $\chi(T)$ of crystals **1**−**4** below and above the magnetic ordering temperature. For the *y* direction at $T < T_N$, $\chi(T)$ was determined from eq 1. As can be seen from Figures 9 and 10, there are anomalies on the curves $\chi(T)$ for the *y* direction in all single crystals. The antiferromagnetic transition temperature T_N was taken to be the value at which $d\chi_M/dT$ is maximal. Table 3 lists the values of T_N and M_S(2 K) for **1**−**4**.

Magnetic Susceptibility above T_N. Above the magnetic transition temperature, there is a wide maximum on the curve $\chi(T)$, which is clearly seen in Figure 9. As mentioned above, this maximum is due to antiferromagnetic ordering in the exchange cluster >N−•O···H−O^R−Ni^{2+}−RO−H···O•−N< preceding the magnetic phase transition. The temperature of the broad maximum (T_{max}) is directly related to the exchange interaction energies in this exchange cluster. A decrease in T_{max} from 18 K for **1** to T_{max} < 4 K for **4** on the curves $\chi(T)$ (Table 3) indicates that the exchange interaction energies J_2 decrease

(20) Ikorskii, V. N.; Romanenko, G. V.; Sygurova, M. K.; Ovcharenko, V. I.; Lanfranc de Paunthou, F.; Rey, P.; Reznikov, V. A., Podoplelov, A. V.; Sagdeev, R. Z. *Zh. Strukt. Khim.* **1994**, *35*, 76.
(21) Ovcharenko, V. I.; Ikorskii, V. N.; Vostrikova, K. E.; Burdukov, A. B.; Romanenko, G. V.; Pervukhina, N. V.; Podberezskaya, N. V. *Izv. Sib. Otd. Akad. Nauk SSSR, Ser. Khim. Nauk* **1990**, *5*, 100.
(22) Ovcharenko, V. I.; Romanenko, G. V.; Korobkov, I. V.; Ikorskii, V. N.; Ovcharenko, I. V.; Musin, R. N.; Vostrikova, K. E.; Podoplelov, A. V.; Shishkin, O. V.; Struchkov, Yu. T. *Zh. Strukt. Khim.* **1998**, *39*, 897.
(23) Moriya, T. *Phys. Rev.* **1960**, *120* (1), 91.
(24) Turov, E. A. *Phizitcheskie Svoistva Magnitouporyadotchennykh Kristallov*; Izdatelstvo Akademii Nauk SSSR: Moskva, 1963.

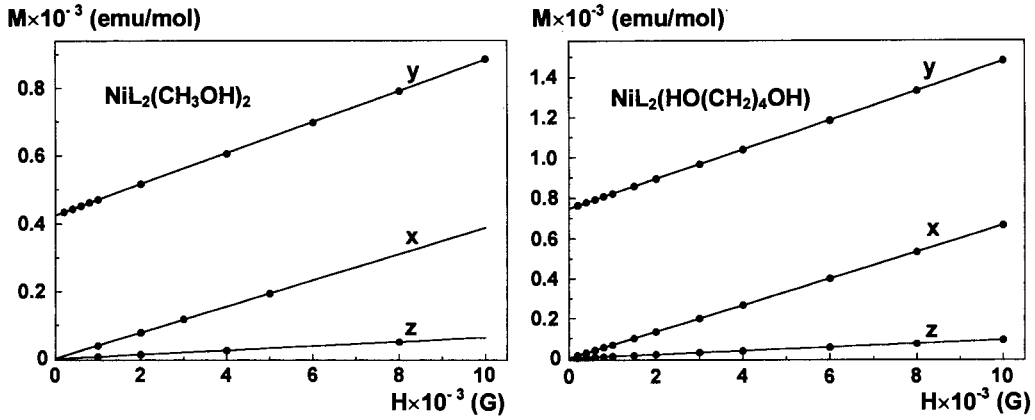

Figure 5. Field dependence of magnetization for single crystals of $NiL_2(CH_3OH)_2$ and $NiL_2(HO(CH_2)_4OH)$ at 2 K.

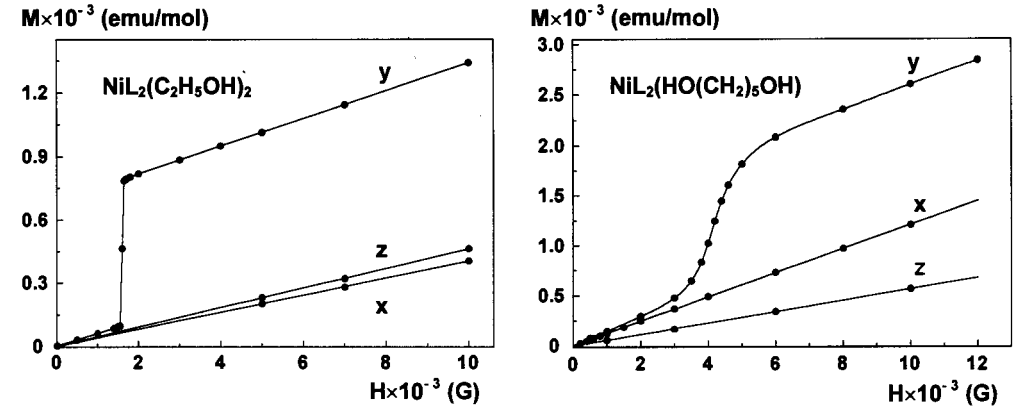

Figure 6. Field dependence of magnetization for single crystals of $NiL_2(C_2H_5OH)_2$ and $NiL_2(HO(CH_2)_5OH)$ at 2 K.

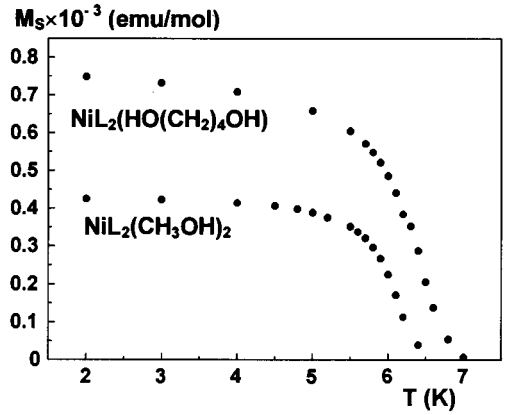

Figure 7. Temperature dependence of spontaneous magnetization for single crystals of $NiL_2(CH_3OH)_2$ and $NiL_2(HO(CH_2)_4OH)$.

on going from **1** to **4**. At the same time, the exchange parameter J_1 must remain virtually unchanged, since this channel of interaction is constant for all crystals. Table 3 gives the optimal values of the effective exchange parameter J estimated by simulating the experimental dependence $\chi(T)$ at $T > T_N$ in the exchange cluster $>N-^{\bullet}O\cdots H-O^{R}-Ni^{2+}-^{R}O-H\cdots O^{\bullet}-N<$.[25] The qualitative character of these calculations is explained by the fact that in **1**−**4** this exchange cluster may not be treated as a strictly isolated cluster ($|J_2| \gg J_1$) as required by the computational cluster model. Therefore, the values of the averaged exchange parameter J derived in this modeling are actually correlated values between J_1, J_2, and J', where J' is the energy of exchange interaction between layers. Since the energy of J_1 exchange interactions is[15,21,22] $\sim+10$ cm^{-1}, we can argue that J_2 is about $(J - 10)$ cm^{-1}.

Magnetic Ordering. The main difference of the magnetic structures of crystals **1**, **3** from those of **2**, **4** lies in the fact that in **1**, **3** the most energetically favorable state of crystals is the antiferromagnetic state with weak ferromagnetism. In **2**, **4,** the ground state is purely antiferromagnetic and the state with weak ferromagnetism is only induced by an external magnetic field. The symmetry of this crystalline structure admits the pure antiferromagnetic state when the structure is ordered along the *y* axis, and the weakly ferromagnetic state is possible when the structure is ordered along the *z* axis.[24] In the latter case, the ferromagnetic moment must be directed along the *y* axis. For analyzing the magnetic structure of the crystals, it is convenient to divide the system of magnetic centers into four magnetic sublattices. These are two sublattices of nickel atoms Ni1 and Ni2 and two sublattices of R1 and R2 radicals belonging to two types of molecules in nonequivalent positions (Figure 2a). It is noteworthy that the R1 and R2 sublattices include pairs of radicals bonded to the Ni(II) ion from the Ni1 and Ni2 sublattices. Since the total spin of the two radicals equals the spin of the Ni(II) ion in each molecule, the magnetic moments of Ni1 and R1, Ni2 and R2 sublattices are close in magnitude (as shown schematically in Figures 11 and 12).

An analysis of the experimental magnetic susceptibility curves $\chi(T)$ below T_N permits one to draw certain conclusions about the ordering of magnetic moments in **1**−**4**. Figure 9 shows the curves $\chi_\alpha(T)$ ($\alpha - x, y, z$) for **1** and **3**; it can be seen that only $\chi_z(T)$ tends to zero at $T \rightarrow 0$ for both compounds. This means that the magnetic moments of the nickel ions (Ni1 and Ni2 sublattices) and nitroxides (R1 and R2 sublattices) are ordered along this direction (Figure 11a), and the measured magnetic

(25) Gelman, A. B.; Ikorskii, V. N. *Koord. Khim.* **1988**, *14*, 491.

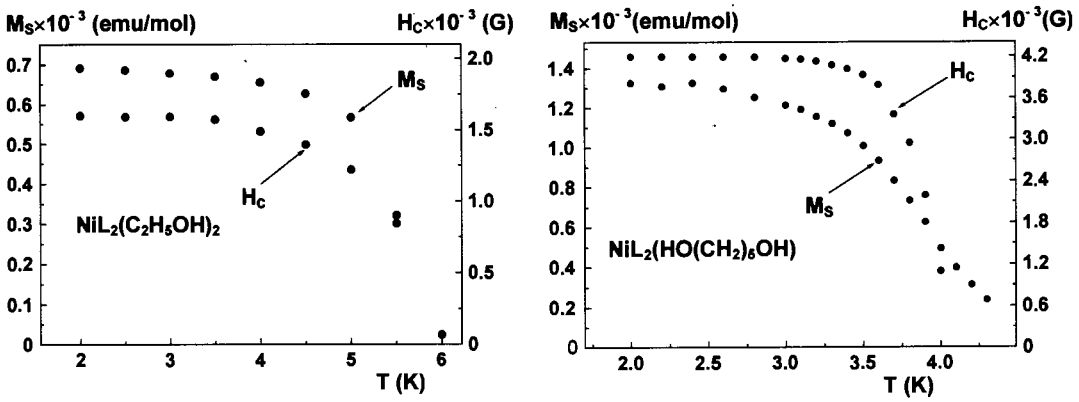

Figure 8. Temperature dependencies of spontaneous magnetization and the critical magnetic field for a single crystals of $NiL_2(C_2H_5OH)_2$ and $NiL_2(HO(CH_2)_5OH)$.

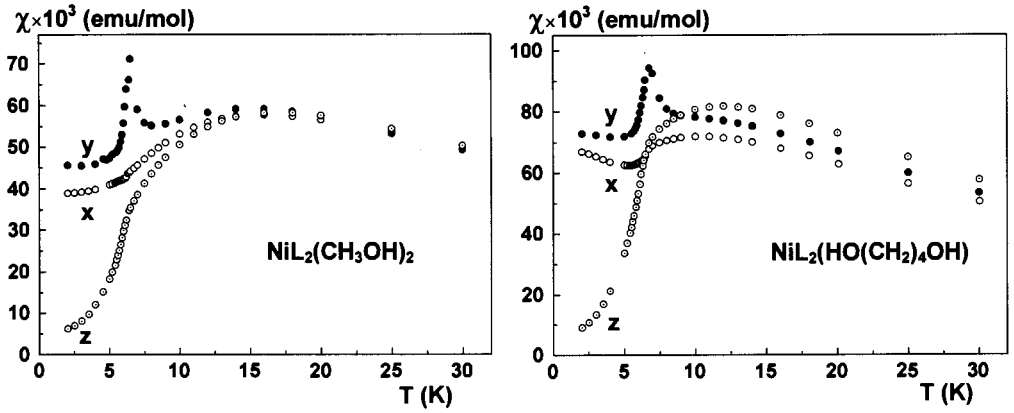

Figure 9. Temperature dependencies of magnetic susceptibility for single crystals of $NiL_2(CH_3OH)_2$ and $NiL_2(HO(CH_2)_4OH)$.

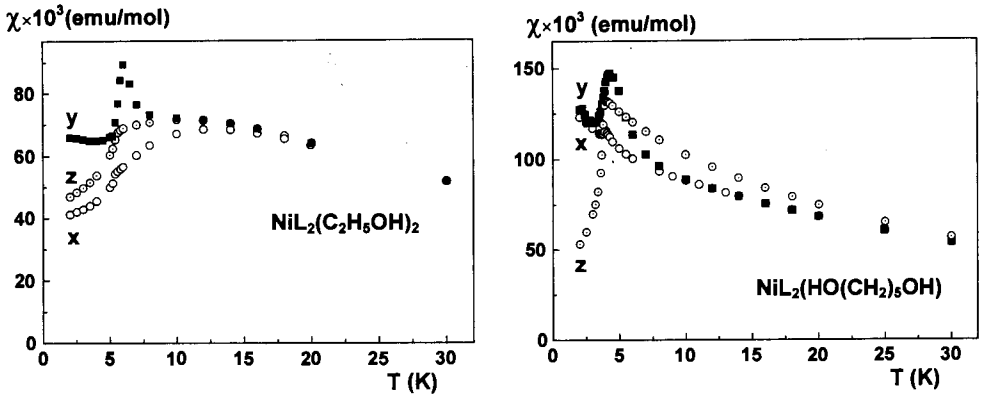

Figure 10. Temperature dependencies of magnetic susceptibility for single crystals of $NiL_2(C_2H_5OH)_2$ and $NiL_2(HO(CH_2)_5OH)$.

Table 3. Magnetic Parameters for **1**−**4**

compound	T_N, K ±0.05	M_S, emu·mol^{-1} ± 5	$-J$, cm^{-1} ±0.3
1	6.5	435	6.9
2	5.3	691	6.0
3	6.8	756	5.5
4	4.0	1338	2.7

susceptibility is $\chi_{||}$. In the other two directions (x and y), the perpendicular component of magnetic susceptibility $\chi_{\perp}(T)$ is measured; as would be expected, $\chi_{\perp} > \chi_{||}$. In this case, the ferromagnetic moment is directed along the y axis. Thus for crystals **1** and **3**, one can imagine two alternative models of magnetic ordering, which are very similar in character (Figure 11). The insignificant difference between the models lies in the fact that one of them reflects the situation with the weak ferromagnetic moment formed by tilting only nickel sublattices (Figure 11a) and the other shows formation of the weak ferromagnetic moment by both paramagnetic systems (Figure 11b). It is most important for us that the weak ferromagnetic moment is directed along the 2-fold symmetry axis, in conformity with classical theory of magnetism.

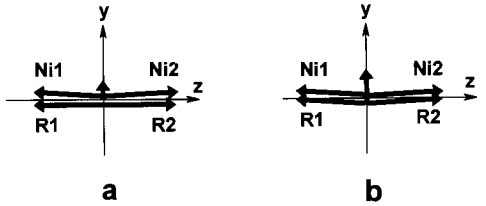

Figure 11. Scheme of magnetic ordering in single crystals of **1** and **3**.

For crystals **2** and **4**, the situation is much more complicated. When the measurements are performed in weak fields along the principal axis of antiferromagnetism y, $\chi_y < \chi_x, \chi_z$, if the

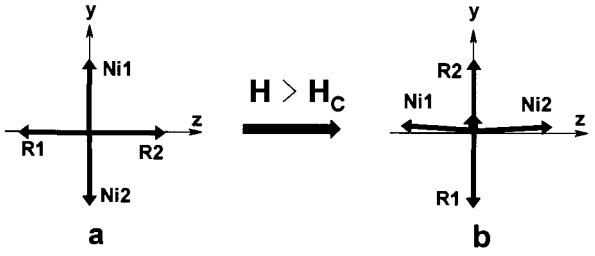

Figure 12. Scheme of magnetic ordering in single crystals of **2** and **4**.

magnetic moments of all magnetic sublattices are ordered in this direction. The longitudinal component of magnetic susceptibility $\chi_y(T) \equiv \chi_{II}(T)$ must tend to zero when the temperature decreases. However, as can be seen from Figure 10, this condition is not fulfilled. This situation takes place if we assume that only the magnetic moments of nickel ions are ordered antiferromagnetically along the *y* axis, whereas the magnetic moments of the unpaired electrons of nitroxyl groups are ordered antiferromagnetically along the transverse *z* direction. In this case, transverse magnetic susceptibility $\chi_\perp$ of the magnetic moments of nitroxides is measured along with longitudinal magnetic susceptibility χ_{II} along the *y* axis of antiferromagnetically ordered magnetic nickel ions (Ni1 and Ni2). As a result, the magnetic structure of the ordered phase in weak fields for crystals **2** and **4** may be represented as a cross (Figure 12a). When the magnetic field exceeds the critical value, a spin flop type transition occurs, during which the antiferromagnetically ordered magnetic moments of nickel ions turn in the *z* direction and a weak ferromagnetic moment appears. This must be accompanied by a sharp increase in magnetic susceptibility χ, determined from eq 1 (i.e., by an increase in the tangent of the slope in Figure 6), since the spin flop changes χ_{II} to $\chi_\perp$ in the nickel subsystem. However, this does not take place; from Figure 6 it is clear that the tangents of the slope of the lines $M_y(\mathbf{H})$ for $\mathbf{H} < \mathbf{H}_C$ and $\mathbf{H} > \mathbf{H}_C$ are almost the same. Based on the data for single crystals **2** and **4**, it is reasonable to assume that, when $\mathbf{H} > \mathbf{H}_C$, the spin flop takes place simultaneously in the nickel magnetic subsystem and in the nitroxide subsystem (Figure 12b). As a result, the weak ferromagnetic moment for these crystals is formed due to the slope of only nickel subsystems.

Conclusions

In conclusion, using hydrogen bonds may be an effective technique in the design of heterospin molecular magnets based on complexes of transition metals with nitroxides. In **1**−**4** formation of tight hydrogen bonds O···HO between the coordinated OH groups of alcohol molecules and the N−•O groups of ligands L leads to formation of layers in the solids. It is important to note that hydrogen bonds not only promote formation of systems with high structural dimensionality but even create effective exchange channels. In **1**−**4**, such channels are >N−•O···H−O^R−Ni^{2+}−^{R}O−H···O•−N< fragments. A comparison of the magnetic properties of **1**−**4** with those of isostructural $NiL_2(H_2O)_2$ described earlier and not possessing an ability of magnetic ordering[15] leads to a paradoxical conclusion that saturation of the compound with an organic component (i.e., substitution of the hydrogen atom in the water molecule by the hydrocarbon radical in passing from $NiL_2(H_2O)_2$ to **1**−**4**) is favorable for magnetic ordering of spins. However, for the design of molecular ferromagnets based on metal compounds with organic ligands, this situation seems to be quite natural, because replacement of the electron-accepting proton by the electron-donating hydrocarbon radical R in the exchange channel >N−•O···H−O^R−Ni^{2+} considerably increases the energy of exchange interactions between the unpaired electrons of the paramagnetic centers.

In their magnetic behavior, the heterospin compounds investigated fall into two groups: **1**, **3** and **2**, **4**. Two types of magnetic phase transitions to the weakly ferromagnetic state were recorded, which depends on the alcohol molecule of the compound; one transition (for **2** and **4**) is induced by the external magnetic field. This result correlates with an increase of Ni−O(01) and O(01)...O(011′) distances in **2** and **4** by 0.01−0.02 and 0.05−0.13 Å relative to **1** and **3**, respectively (Table 2). Since the Ni−O(01) and O(01)...O(011′) bonds enter into the >N−•O···H−O^R−Ni^{2+} exchange channel, their lengthening is not favorable for cooperative ordering of spins. As a result, the weak ferromagnetic ordering in **2** and **4** takes place at lower temperatures than for **1** and **3** (Table 3) and in magnetic fields above critical. The difference in the character of ordering in **1**, **3** and **2**, **4** (Figures 11 and 12) shows how significantly the magnetic properties of molecular ferromagnets can change even with minor structural changes in exchange channels.

It should be noted that ordering of magnetic subsystems in **1**−**4** actually takes place within polymer layers. Drawing the layers apart, i.e., an increase in interlayer distances (Table 2) on passing from **1**, **2**, to **3** and especially to **4** does not affect the magnetic ordering ability of the compounds. The data obtained do not reveal any tendency in variation of the magnetic properties of the compounds that is due to a significant increase in F···F interlayer contacts from 2.875 for **1** up to 4.176 Å for **4**. As a result, substitution of alcohols by glycols led to a change in structural dimensionality, i.e., to a transition from layered to frame structures and increased stability of the compounds but did not change the "magnetic" dimensionality of the compounds in the sense that magnetic ordering in **1**−**4** occurs only within layers.

Investigating the magnetic properties of single crystals allowed us to reveal the anisotropy of magnetic susceptibility of the compounds and to correlate the direction of the axis of easy magnetization with the crystal structure of the complexes.

Acknowledgment. We are grateful to the Russian Foundation for Basic Research (Grant No. 96-03-32229), Ministry of Science and Technical Policy of Russia, and INTAS (Grant No. 94-3508) for financial support.

Supporting Information Available: Tables, in CIF format, of crystallographic details, atomic coordinates, displacement parameters, and bond distances and bond angles are available on the Internet only. Access information is given on any current masthead page.

IC9801847